ASCE International Journal of Geomechanics. Submitted Feb 2021; Published Dec 2021.
https://doi.org/ 10.1061/(ASCE)GM.1943-5622.0002291

Effect of soil moisture evaporation rate on dynamic measurement of water retention curve with high capacity tensiometer

Meghdad Bagheri[1], Mohammad Rezania[2]

Abstract

This paper investigates the effect of soil moisture evaporation rate on the soil water retention curve (SWRC) of clays obtained using high-capacity tensiometer (HCT) technique and following the continuous drying (dynamic) method. SWRC measurements, with and without soil moisture evaporation rate control, were carried out on reconstituted London clay specimens using 12 performance-improved HCTs recently developed at the University of Warwick. Furthermore, the HCTs' performance in terms of the maximum attainable suction (s_{max}) and maximum measurement duration (t_{max}) was evaluated. Moreover, the suitability of a curve fitting-based model, available in the literature, for attaining the entire retention curve (beyond the capacity of HCTs) was evaluated. The SWRCs for tests with controlled evaporation rate were found to be generally exhibiting higher suctions at a given water content, hence inducing air-entry values that were on average 16% higher than those obtained from tests without evaporation rate control. It was also found that for suctions beyond 2 MPa, the curve fitting-based model predictions of data obtained from tests with controlled evaporation rate exhibit significantly lower suctions at a given water content than those without evaporation rate control, suggesting that such curve fitting correlations should be used with caution.

[1]Lecturer, School of Energy, Construction and Environment, Coventry University, Coventry, UK.
Email: ac6031@coventry.ac.uk. ORCID: https://orcid.org/0000-0002-9748-4165

[2]Reader, School of Engineering, University of Warwick, Coventry, UK. (Corresponding Author)
Email: m.rezania@warwick.ac.uk. ORCID: https://orcid.org/0000-0003-3851-2442

ASCE International Journal of Geomechanics. Submitted Feb 2021; Published Dec 2021.
https://doi.org/ 10.1061/(ASCE)GM.1943-5622.0002291

Author Keywords: High-capacity tensiometer, Soil water retention curve, Evaporation rate, Air-entry value

Introduction

Mechanical behaviour of unsaturated soils is controlled by the pore-water tension (suction) and the ability of the soil for water retention, the latter being characterised as the soil water retention curve (SWRC), which is defined as the continuous and non-linear relationship between the water content (or degree of saturation) and suction (s) in soils during wetting or drying (Fredlund and Rahardjo, 1993). Various experimental methods for development of SWRCs have been reported in the literature including negative water column (Pagano et al., 2016), axis-translation (Bagheri et al., 2020), pressure plate (Noguchi et al., 2012), and high capacity tensiometers (HCT) (Marinho and Teixeira, 2009). Among these, HCTs have recently received significant attention for laboratory measurement of SWRCs of various soil types, thanks to their fast response and short equilibrium time (Bagheri et al., 2019; Rezania et al., 2020).

In the laboratory determination of SWRC using HCTs, one method is to place the soil specimen on a digital balance and expose it to continuous air-drying. The electronic balance simultaneously monitors changes of water content, while the evolution of suction in the continuously drying specimen is recorded by the HCT. This method is known as 'dynamic' method (Lourenço et al., 2011).

The effect of evaporation rate on the SWRC measured by dynamic method was studied by Cunningham (2000) and Boso et al. (2003) respectively on reconstituted silty clay and clayey silt specimens. In the former study, the evaporation rate was controlled in a humidity-controlled chamber, and in the latter study, the evaporation rate was slowed down by wrapping the specimen in a geotextile. Both studies revealed no or little differences between the SWRCs obtained during controlled and uncontrolled evaporation tests. Currently, with very limited

experimental data, there is no clear evidence on whether the evaporation rate has an influence on SWRC measurement using HCTs.

This paper presents the results of SWRC measurements carried out on reconstituted London clay (LC) specimens using the newly developed HCTs at the University of Warwick (denoted WT hereafter). The SWRCs were measured based on the dynamic method, with and without evaporation rate control. A comparison of the obtained SWRCs from these methods along with an analysis of the mathematical curve fitting approach, used to attain the entire retention curve, are presented. Furthermore, the performance of the WTs during SWRC measurements are evaluated.

Test Material and Specimen Preparation

The material used in this study is LC, which was collected from an engineering site in the Isle of Sheppey, UK (Bagheri and Rezania 2021). Initially, the natural samples were oven dried at 105˚ C for 48 hours. The dried samples were then crushed into powder using an automatic mortar and sieved through a 1.18 mm sieve. A soil slurry was made by mixing the powder, containing some coarse-grained peds (or large size clay clusters), with distilled de-aired water at 102% water content, an equivalent of 1.5 times liquid limit (*LL*). Reconstituted samples were prepared by consolidating the soil slurry in a 100 mm diameter Perspex consolidometer. The obtained soil cake was then divided into equal subsamples. Identical test specimens were cored from the subsamples using a 75 mm diameter and 20 mm height oedometer cutting ring. Natural LC contains 98% fine grains leading to air-entry values (AEV) of several megapascals. However, the presence of coarse-grained peds in the prepared soil samples resulted in an AEV of around 250 kPa (Bagheri et al., 2020), allowing for detection of unsaturated states on SWRC within the capacity of the WTs (1.5-2.0 MPa). Table 1 presents the index and physical properties of the test material.

ASCE International Journal of Geomechanics. Submitted Feb 2021; Published Dec 2021.
https://doi.org/ 10.1061/(ASCE)GM.1943-5622.0002291

Table 1. Soil properties

Parameter	Value
Plastic Limit (*PL*)	18%
Liquid Limit (*LL*)	68%
Plasticity Index (*PI*)	50
Specific Gravity (G_s)	2.67
Percentage finer than 2 μm	58%
Percentage finer than 63 μm and coarser than 2 μm	30%
Percentage coarser than 63 μm	12%

Experimental Setup

SWRC measurements were carried out on reconstituted specimens using dynamic method with and without evaporation rate control. A total of 12 WTs were available but only 6 tensiometers were used in this study. Figure 1 shows a schematic diagram of an example WT. What distinguishes these HCTs is the surface polishing techniques employed to reduce the surface roughness of the HCTs' diaphragms in order to minimise the presence of gas nuclei in their water reservoirs. This allows for enhanced cavitation threshold and hence, improved maximum attainable suction (s_{max}) and maximum measurement duration (t_{max}). Face milling, silicon carbide abrasive paper polishing, and diamond paste polishing are the mechanical surface polishing techniques employed to achieve smoother diaphragm surfaces. In addition, hydrophilic coating technique using anti-fog agent, Triton X-100, and Titanium Dioxide materials were also employed to further reduce the diaphragm surface roughness and provide higher water affinity characteristics to the polished diaphragms. Table 2 presents the properties of the selected WTs used in this study (see Bagheri et al. 2018 for more details).

ASCE International Journal of Geomechanics. Submitted Feb 2021; Published Dec 2021.
https://doi.org/ 10.1061/(ASCE)GM.1943-5622.0002291

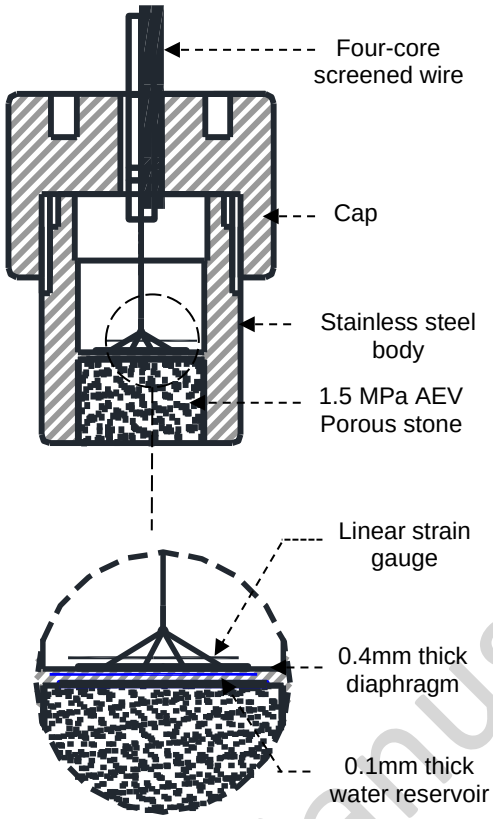

Figure 1. Schematic diagram of WT and its components

Table 2. Properties of the WTs used in this study (data from Bagheri et al., 2018)

HCT	Diaphragm surface treatment	abrev.	s_{max}* (kPa)	t_{max}** (hr)
WT1	Face-milling	FM	972	38
WT4	Silicon carbide abrasive paper polishing	SP	1809	303
WT5	Diamond paste polishing	DP	1838	309
WT8	Hydrophilic coating (anti-fog agent)	AF	1906	300
WT10	Hydrophilic coating (Triton X-100)	TX	1900	412
WT11	Hydrophilic coating (Titanium Dioxide)	TD	2301	529

*In free evaporation tests

**On a specimen with approximately 600 kPa suction

Figure 2 presents the schematic diagram of the experimental setup. For the dynamic method without evaporation rate control, the soil specimen enclosed in the confining ring was placed on a porous stone sitting on the digital balance with a 0.01 g resolution. The porous stone was used to facilitate the continuous drying process by exposing the specimen's base to the atmosphere, hence minimising the effect of exposed surface area. For the dynamic method with evaporation rate control, a perforated chamber was placed around the specimen in order to minimise the air flow over the exposed surfaces, and hence, lowering the soil moisture evaporation rate. Using a mini augur, two holes of 10 mm diameter and 6 mm depth were created on the sample surface to accommodate the HCTs. A spacing of 40 mm was considered between the centrelines of the HCTs. These holes provide lateral support for the probes' body to keep them in place throughout the measurements. This method is believed to reduce the specimen disturbance at the contact area with the tip of the HCT, in comparison with the method followed by Lourenço et al. (2011) and Noguchi et al. (2012) to push the probe 2-3 mm into the specimen, which can cause local consolidation and therefore affect the measurements. Moreover, using the suggested method, suction is measured close to the middle height of the specimen where it can be reasonably assumed that evaporation takes place at a constant and uniform rate. This way the effect of non-uniform evaporation at the exposed surfaces is eliminated. In addition, this method allows for elimination of the accelerated drying in localised areas due to the surface cracking during continuous drying, which can result in development of inhomogeneous suction fields across the specimen. Two HCTs, preconditioned following the procedure explained in Bagheri (2018), were gently fitted into the holes on the specimen surface. A thin layer of soil paste, made by mixing LC powder with distilled de-aired water, was also applied to the tip of the sensor to ensure a good contact with the soil. The sensor cable was also supported by a hanger to eliminate the possible mass measurement errors associated with its weight and stiffness. Measurements of the specimen's mass were

continuously recorded on a computer using an RS232 interface. All of the tests were conducted in a small, environmentally controlled and well isolated room where there is minimal fluctuations of temperature and relative humidity.

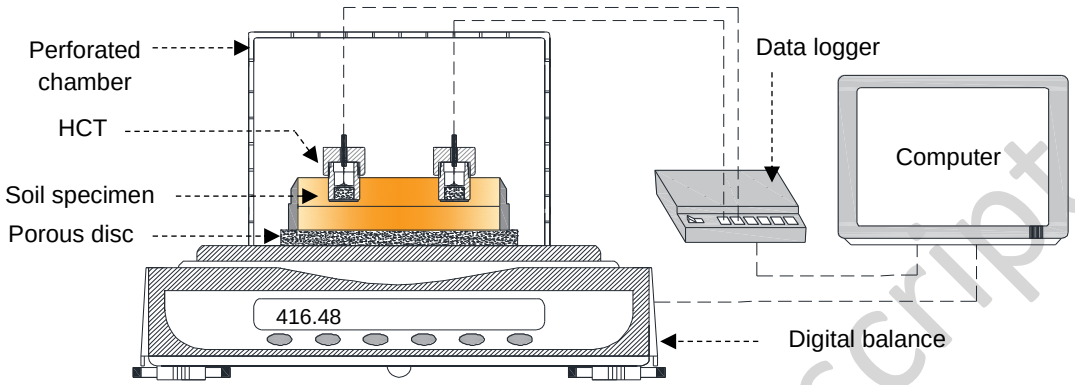

Figure 2. Schematic drawing of the experimental setup for SWRC measurement

Experimental Program

The testing program was carried out under controlled room temperature of 21 ± 1 °C and mean relative humidity of 35 ± 2%. In this set of experiments, only the main drying branch (starting from the fully saturated sate) of the SWRC was produced. The data plotted in gravimetric water content versus suction domain, as the gravimetric water content is the measure usually used in geotechnical engineering practice (Toll et al., 2015). The s_{ae} values were derived based on the intersection point of the tangent lines drawn to the saturated and transition portions of the curve in the semi-logarithmic w – s space. Other more complex methods for derivation of s_{ae} values could be used (e.g. Pasha et al., 2016). However, in order to develop experimental techniques that are both simple, economic, and reliable, the proposed methods for testing and parameters derivation were also kept simple.

Dynamic Tests without Evaporation Rate Control

A total of three tests were performed on initially saturated specimens subjected to air-drying, with two HCTs recording suction evolutions in each specimen. These tests are denoted with DTa-b-XY, with DT standing for dynamic test, 'a' representing the test number, 'b' representing the number of the HCT used (1 to 12), and 'XY' indicating the method used for polishing the HCT's diaphragm. The initial conditions of the specimens as well as the obtained key parameters from DT tests are shown in Table 3. Note that e_0 is the initial void ratio, w_{sat} and w_f are respectively the initial (saturated) and final water contents, Δm_w is the evaporated mass of water, Δt is the test duration, and $\Delta m_w/\Delta t$ is the average moisture evaporation rate.

Table 3. Results of DT tests

Test No.	HCT	e_0	w_{sat} (%)	w_f (%)	Δm_w (g)	Δt (h)	$\Delta m_w / \Delta t$ (g/h)	s_{ae} (kPa)	s_{max} (kPa)
DT1	WT1	1.06	39.72	28.47	12.92	25.3	0.51	210	952
	WT4			26.44	15.25	29.9		208	1601
DT2	WT5	1.05	39.14	26.48	14.50	30.2	0.48	227	1584
	WT8			26.68	14.27	29.7		209	1498
DT3	WT10	1.06	39.67	27.51	14.55	26.5	0.55	244	1510
	WT11			26.12	16.17	29.4		248	1946

Dynamic Tests with Evaporation Rate Control

In reality, the drying process in shallow depth soil layers does not normally take place instantly and over a short period of time. The change in humidity and temperature in the field is a time-dependent process that can be extended over the entire dry season. This process is often interrupted with the rainfalls and climate variations. This is believed to modify the *in-situ* water

retention behaviour of soils compared to the one measured in laboratory using continuous drying procedure. To further study this effect, a series of tests were conducted on the soil specimens subjected to prolonged drying. As shown in Figure 2, a perforated chamber was placed over the specimen to reduce the evaporation rate. The chamber allows for controlled circulation of air around the specimen providing a relatively uniform moisture loss from the top and bottom of the specimen. Three tests were carried out on reconstituted specimens. For each test, two HCTs were used to monitor the evolution of suction as the specimen dried out. These tests are denoted DTEa-b-XY, with 'E' indicating the test was carried out under controlled evaporation rate. The initial conditions of the specimens as well as the obtained key parameters are shown in Table 4.

Table 4. Results of DTE tests

Test No.	HCT	e_0	w_s (%)	w_f (%)	Δm_v (g)	Δt (h)	Δm_v / Δt (g/h)	s_{ae} (kPa)	s_{max} (kPa)
DTE1	WT1	1.05	39.34	30.54	10.14	63.4	0.16	252	908
	WT4			27.16	14.07	85.9		263	1580
DTE2	WT5	1.06	39.79	27.40	12.45	73.2	0.17	251	1603
	WT8			28.51	11.33	66.7		263	1312
DTE3	WT10	1.06	39.64	27.55	12.13	71.3	0.17	284	1471
	WT11			26.15	13.81	81.3		265	1893

Results of SWRC Measurements

Figure 3 shows a plot of gravimetric water content and suction against time for DT2 test which shows the decrease of gravimetric water content with time is nearly linear (R^2 = 0.9994). The average moisture evaporation rate for DT tests were estimated in the range of 0.48-0.55 g/h

(Table 3) corresponding to average moisture content change in range of 0.43-0.46 %/h (Figure 4a). The average moisture evaporation rate for DTE tests were estimated in the range of 0.16-0.17 g/h (Table 4) corresponding to average moisture content change ranging between 0.14-0.15 %/h (Figure 4b).

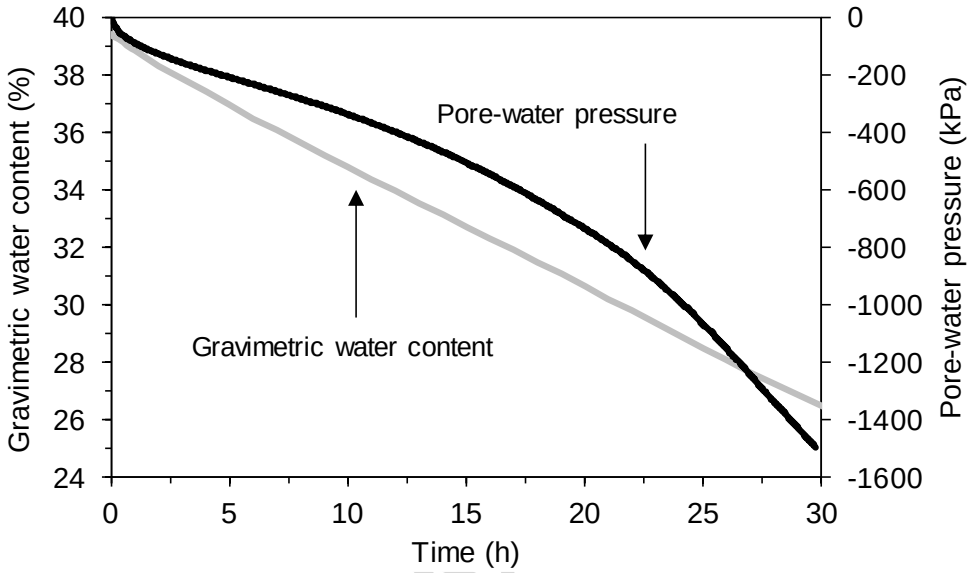

Figure 3. Variation of suction and water content with time for a DT test.

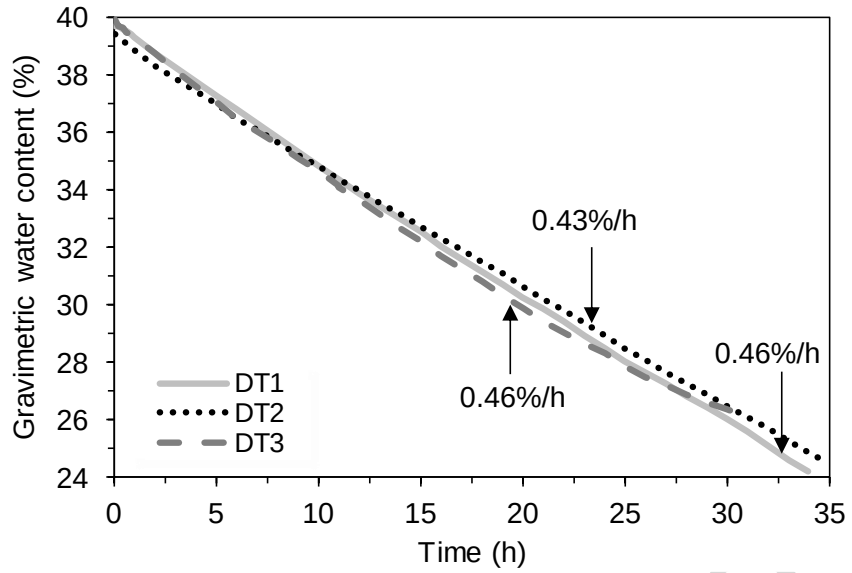

(a)

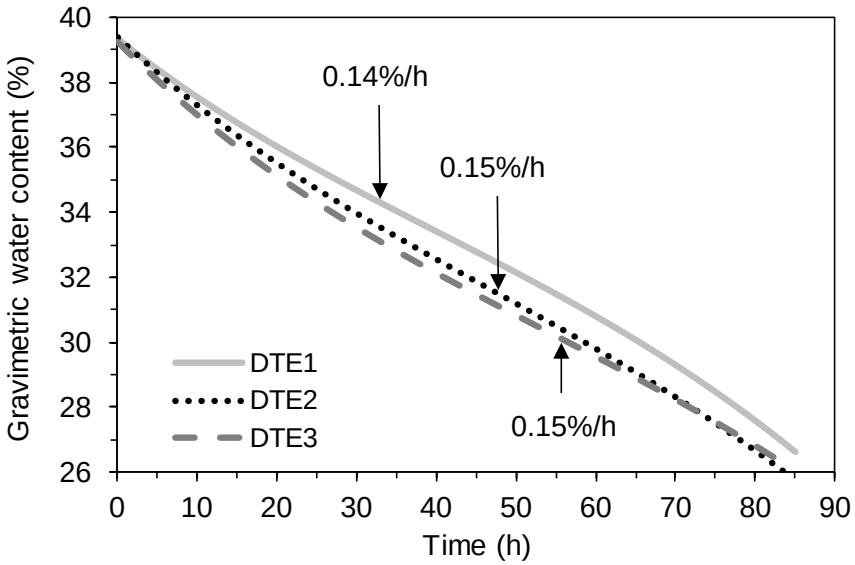

(b)

Figure 4. Variation of water content with time: (a) DT tests; (b) DTE tests

Figures 5 presents the obtained SWRCs from DT and DTE tests. Overall, the two HCTs placed on each specimen recorded similar trends with the main difference being the obtained s_{max} values.

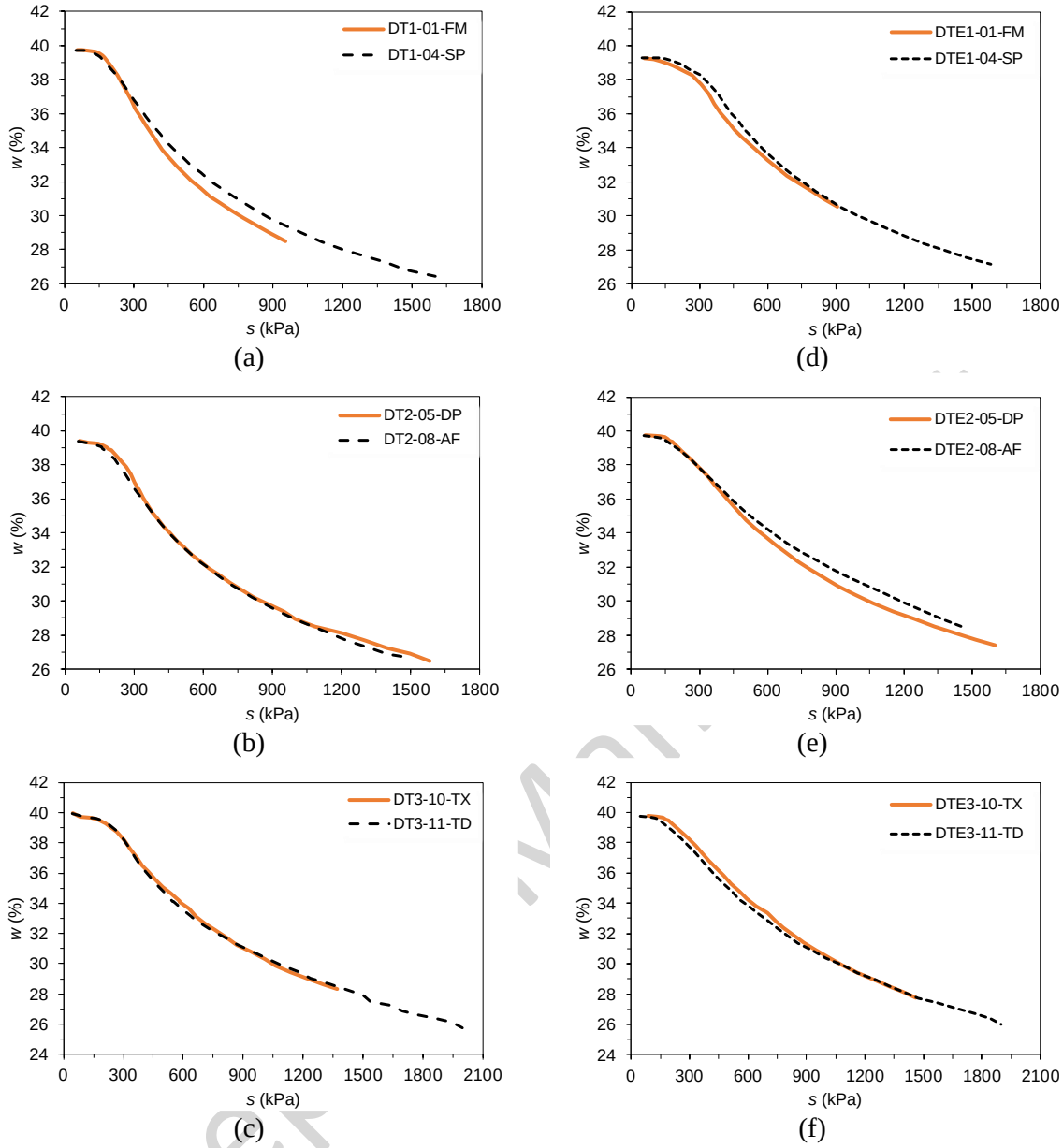

Figure 5. SWRCs obtained from HCT measurements: (a) DT1; (b) DT2; (c) DT3; (d) DTE1; (e) DTE2; and (f) DTE3

Figure 6 presents a comparison of SWRCs obtained by each HCT during both DT and DTE tests. Also shown in Figure 6, are the microscopic images obtained from the profilometry analysis as well as the surface roughness parameter (R_a) obtained for each surface polishing technique applied to the diaphragm of the HCT (see Bagheri et al., 2018). It is seen that the SWRCs for DTE tests are generally shifted to the right, exhibiting higher suctions at a given water content. These shifts are more evident for measurements recorded by FM, SP, DP, and

AF tensiometers. This observation is deemed to be partly due to the fact that during DTE tests the HCTs and the soil specimen had more time to reach equilibrium (although the ultimate equilibrium conditions may not be reached), hence recording higher suctions for a fixed water content. The performance of the TX and TD tensiometers were found to be relatively similar during DT and DTE tests, with main difference being in the measured s_{ae}. Generally, the presence of gas nuclei in the HCT's water reservoir can interrupt the process of pressure transmission from the porous disc (soil-sensor interface) to the pressure measurement device. The similarity in measurements recorded by TX and TD tensiometers during DT and DTE tests can be due to the reduced surface roughness and enhanced hydrophilicity of these two HCTs' diaphragms and the presence of less gas nuclei in their water reservoirs that allowed for uninterrupted pressure transmission. As it is observed in Figures 4(e) and 4(f) that SWRCs from DT and DTE tests overlap each other to a high degree, it can be concluded that the effect of increased hydrophilicity in TX and TD tensiometers almost supersede the effect of evaporation rate control in the timescale of DTE tests. This is an interesting observation and could be matter of further investigations.

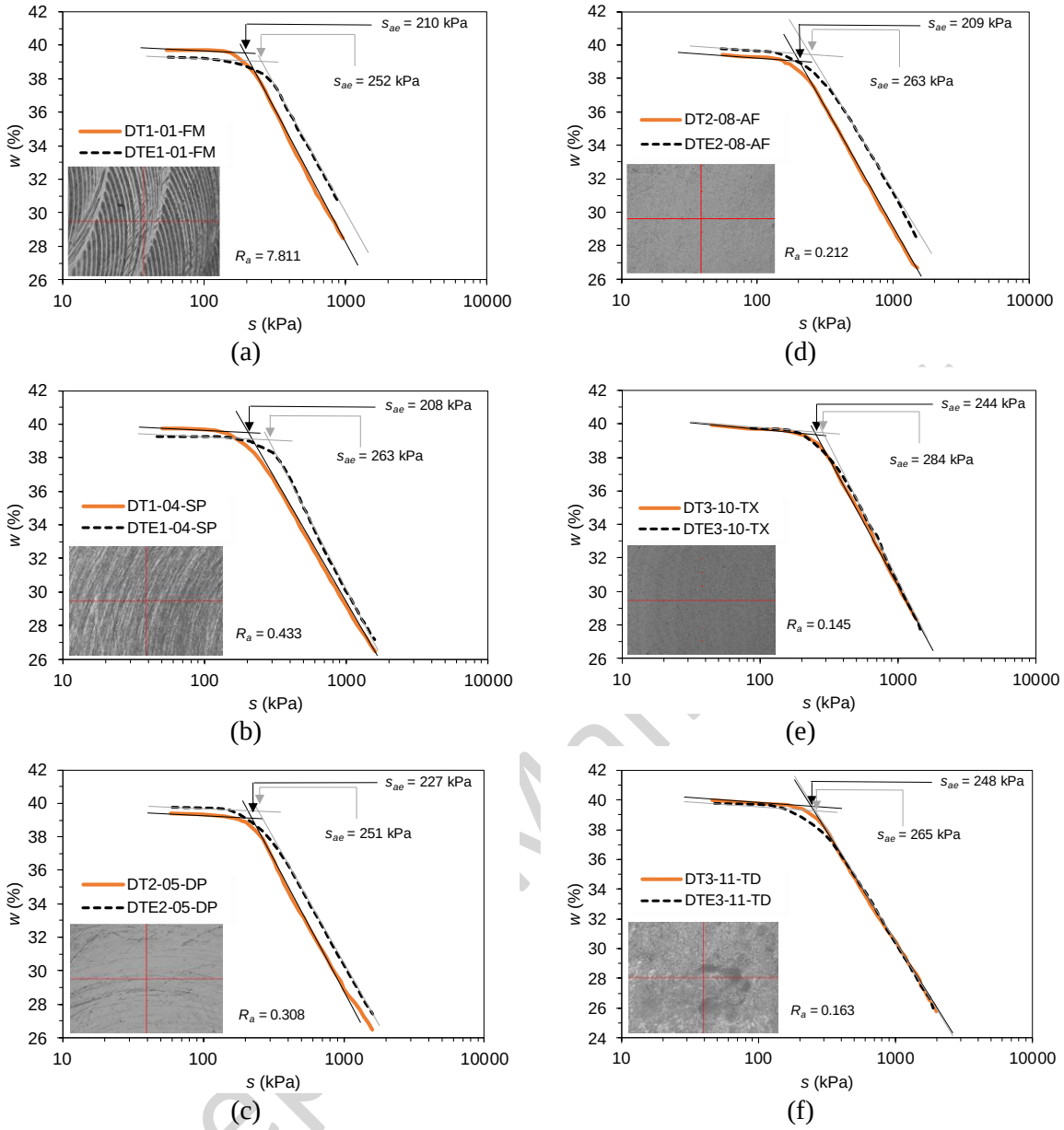

Figure 6. Comparison of SWRCs obtained from DT and DTE tests for different HCT types: (a) FM; (b) SP; (c) DP; (d) AF; (e) TX; and (f) TD

It must be noted here that the presented SWRCs relate local suction to global water content. In fact, suction distribution at the mid-height of the tested specimens might be different, resulting in slightly different SWRCs. Moreover, suction measurements were carried out under non-equilibrium conditions, i.e. where the soil and the HCT were not in ultimate equilibrium. These can help explaining the differences observed in SWRCs obtained from DT and DTE tests.

HCTs' Performance

Comparison of s_{max}, s_{ae}, and t_{max} in DT and DTE tests

A comparison of the s_{max} values recorded during DT and DTE tests is shown in Figure 7. Also shown in the figure is the free evaporation (FE) test results, reported in Bagheri et al. (2018), in which the tensiometer, pre-pressurised at 4 MPa positive pressure in a saturation chamber, was placed in free water for pressure equilibrium and then the ceramic filter was wiped and allowed to dry off at ambient temperature until cavitation occurred.

All HCTs showed significantly lower s_{max} values during DT and DTE tests than the FE tests. It was also observed that the change in soil moisture evaporation rate did only have a minor impact on the recorded s_{max} values during DT and DTE tests. The prolonged contact of the HCTs with the unsaturated specimen during DTE tests, resulted in a slight reduction of the recorded s_{max} values, with differences being generally in a range of 20 – 50 kPa (with exception of WT8 in Figure 7). Furthermore, all performance-improved HCTs recorded s_{max} values approximately equal or higher than the nominal capacity of the WT (1.5 MPa) during DT tests. This is while the limited data reported in the literature on dynamic SWRC measurement of fine-grained soils (without evaporation rate control) using HCTs reveal that, for all cases, the recorded s_{max} values were lower than the nominal capacity of the utilised tensiometers (Figure 8). These data, presented in a normalised water content (w/w_0) against suction plot, include SWRC measurement of a loess material using CERMES HCT (Munoz-Castelblanco et al., 2012), a compacted sandy clay from BIONIC embankment using Wekeham Farrance – Durham (WF-D) tensiometer (Lourenço et al., 2011), a compacted kaolin clay using an integrated HCT (Chen et al., 2015), and a sandy clay soil using WF-D HCT (Toll et al., 2015). This may further support the appropriateness and usefulness of the performance improvement

technique of reducing the diaphragm surface roughness and hydrophobicity in attainment of higher suction ranges during dynamic SWRC measurements.

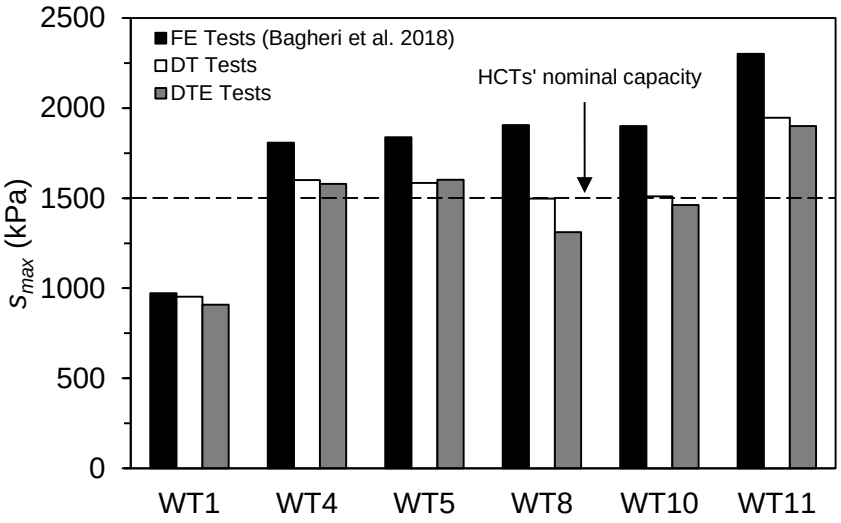

Figure 7. Performance of HCTs in terms of s_{max} during FE, DT, and DTE tests

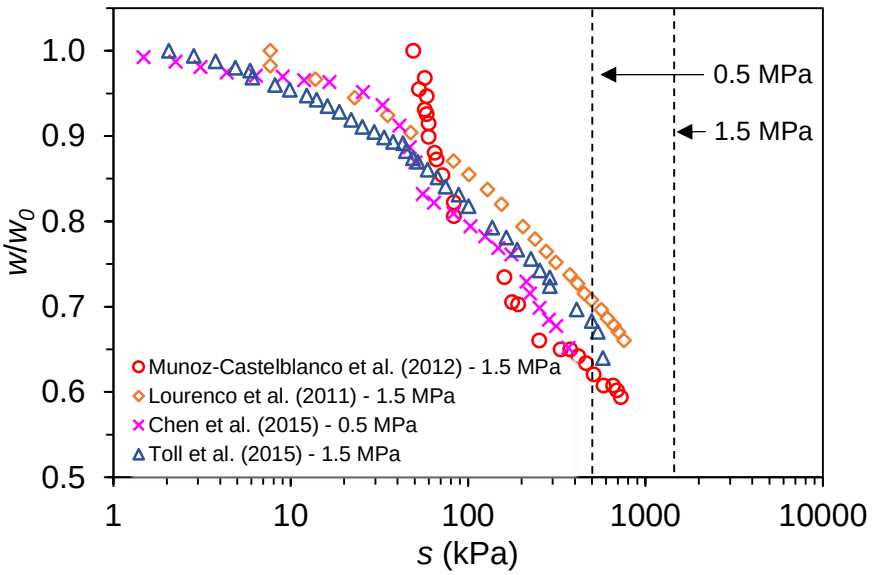

Figure 8. Drying-path SWRC of fine-grained soils determined using HCTs and following continuous drying method

Figure 9 presents a comparison of the s_{ae} values derived from DT and DTE tests. The two HCTs placed on the same specimen generally recorded close s_{ae} values with a mean difference of

approximately 8 kPa for DT tests and 12 kPa for DTE tests. This mean difference is increased to approximately 39 kPa for measurements made by each HCT during DT and DTE tests.

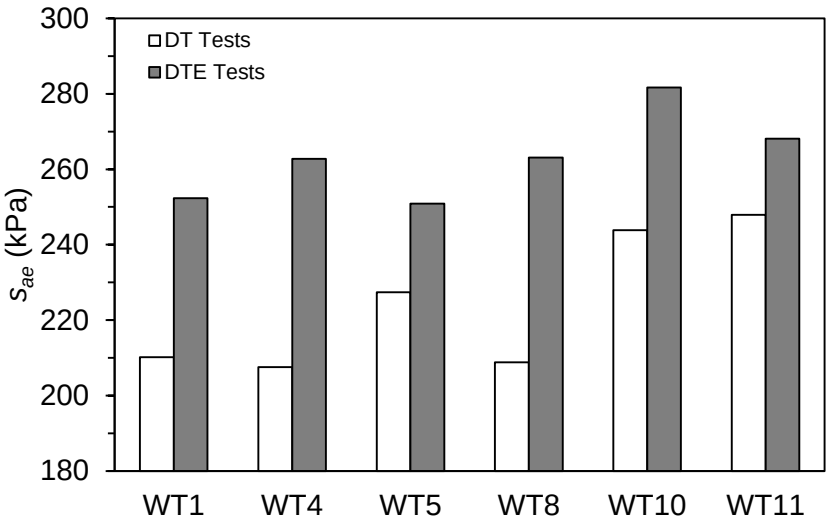

Figure 9. Comparison of s_{ae} values obtained from DT and DTE tests

Figure 10 presents a comparison of the t_{max} values recorded during DT and DTE tests. Clearly, the HCTs recorded higher t_{max} values during DTE tests with controlled evaporation. With evaporation rate during DTE tests being approximately 3 times slower than DT tests (see Tables 3 and 4), the mean t_{max} value obtained during DTE tests was 2.6 times higher than DT tests. Similar to s_{max} and s_{ae} values obtained during DT and DTE tests, no trends could be found in recorded t_{max} values.

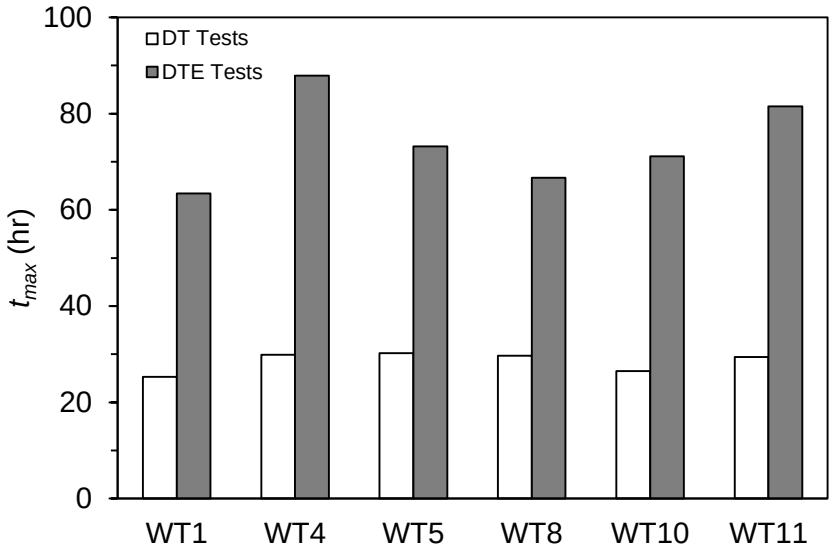

Figure 10. Performance of HCTs in terms of t_{max} during DT and DTE tests

Discussion

Explaining the differences observed in measurement of s_{max} and t_{max} values during DT and DTE tests requires a thorough understanding of the main factors contributing to cavitation in HCTs. These factors can be outlined as the size and particle size distribution of the porous ceramic, (2) the size of the water reservoir, (3) the surface roughness of the diaphragm on the reservoir side, and (4) the saturation and pre-conditioning procedure followed.

One possible reason for observation of different t_{max} values in DT and DTE tests can be due to the effect of air diffusion and occurrence of cavitation inside the ceramic filter at suctions below or close to the ceramic's AEV during the prolonged contact with the soil specimen. With increased contact of the ceramic filter with the unsaturated soil, the very small air (gas) cavities pre-existed in the porous stone start to grow in size. On the other hand, as the soil specimen dries out the air phase prevails the water phase increasing the possibility of continuous air passages developing at the soil-filter interface, facilitating the air diffusion and trigger of cavitation. Control of evaporation rate delays the process of specimen desaturation and transition from quasi-saturated state (discontinuous air phase) to partially saturated state

(continuous air and water phase) and finally to the residual state (discontinuous water phase). The tiny gas cavities within the ceramic disc also receive the energy required for their expansion and formation of continuous air phase in a delayed mode. The delay in air diffusion process results in observation of higher t_{max} values during DTE tests. The higher measurement duration does not necessarily entail higher maximum attainable suction. The increased number of gas bubble formations may lower the energy required for expansion of the remaining entrapped air inside the porous ceramic and trigger early cavitation. Similar reasoning may be considered in explaining the higher s_{max} values observed in FE tests than in the DT and DTE tests. In contrast to FE tests, in the dynamic tests the ceramic filter is in contact with soil containing undissolved air bubbles in the pore-water. The water exchange between the ceramic filter and soil's pore-water results in transfer of these air bubbles to the porous ceramic, and possibly the water reservoir, triggering cavitation at lower suction values than that of observed in FE tests.

It is worth mentioning here that the air diffusion process depends on the AEV and the hydraulic conductivity of the porous ceramic, which are, in turn, directly influenced by the ceramic's porosity. The porosity of the ceramic filter varies according to the size and distribution of the pores. As shown in the micrographs of Figure 11, the size and distribution pattern of the pores of ceramics are not uniform and pores exhibit irregular formation patterns.

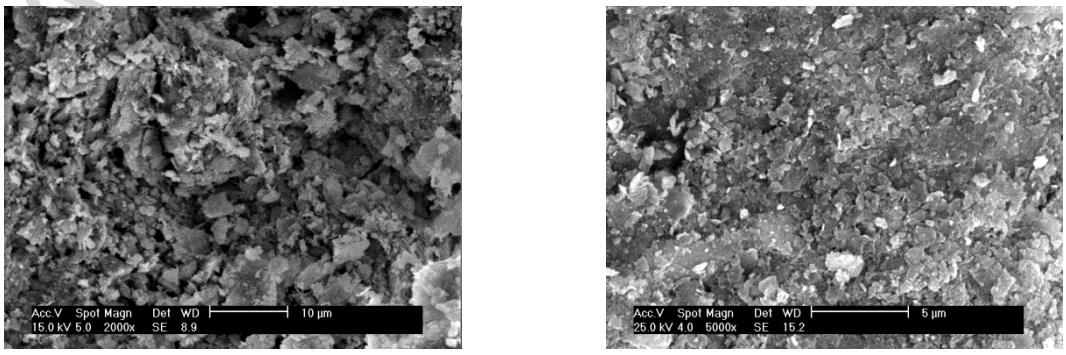

(a) (b)

Figure 11. SEM micrographs of the porous ceramic at magnifications of: (a) 2000x; (b) 5000x

Cavitation may also trigger inside the water reservoir of HCTs. As shown in Figure 12(a), the initially trapped air bubble inside a large crevice on the water reservoir wall grows as the water tension magnitude is increased. Having received enough tension pressure, the bubble is released from the crevice, causing cavitation in the water reservoir. Reducing the size and the number of crevices, and hence, the size and the number of entrapped gas bubbles, as well as increasing the hydrophilicity of the diaphragm wall on the reservoir side can significantly increase the energy required for formation of free gas bubbles (Figure 12b,c).

The mechanism of cavitation in HCTs is complex; it is not clear when, and how the cavitation occurs, whether it is initiated in the water reservoir or in the ceramic disc, and that which one is predominant.

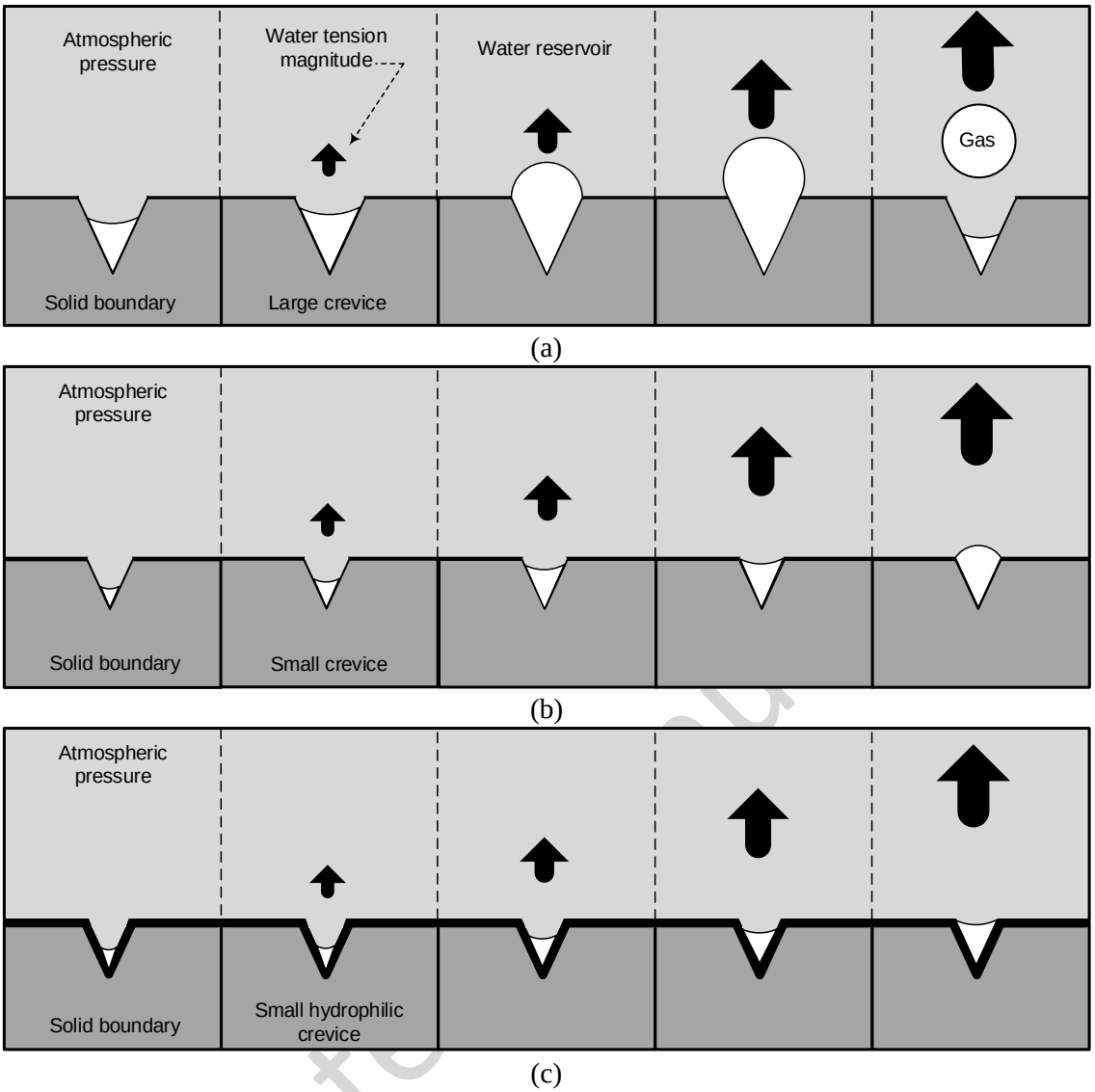

Figure 12. Cavitation inside the water reservoir: (a) large crevice; (b) small crevice; (c) small hydrophilic crevice

Mathematical Curve Fitting to SWRC Data

Measurement of SWRC using HCTs is limited to the s_{max} value that is typically less than 2 MPa. In order to extend the SWRC to a wider suction range one method is to use sigmoidal curve fitting equations to mathematically extrapolate the variation of water content with soil suction where the data points for high suctions are not available. Several equations have been so far proposed in the literature. One of the most widely used set of curve fitting equations is the one proposed by Fredlund and Xing (1994);

ASCE International Journal of Geomechanics. Submitted Feb 2021; Published Dec 2021.
https://doi.org/ 10.1061/(ASCE)GM.1943-5622.0002291

$$w(s) = w_{sat}\left[1 - \frac{\ln\left(1+\frac{s}{s_r}\right)}{\ln\left(1+\frac{10^6}{s_r}\right)}\right] \times \left[\frac{1}{\ln\left[\exp(1)+\left(\frac{s}{a}\right)^n\right]}\right]^m \quad (1)$$

$$m = 3.67\ln\left[\left(\frac{w_{sat}}{w_i}\right) \times \left(1 - \frac{\ln\left(1+\frac{s_i}{s_r}\right)}{\ln\left(1+\frac{10^6}{s_r}\right)}\right)\right] \quad (2)$$

$$n = 3.72s' \frac{1.31^{m+1}}{m \times \left(1 - \frac{\ln\left(1+\frac{s_i}{s_r}\right)}{\ln\left(1+\frac{10^6}{s_r}\right)}\right)} \quad (3)$$

$$s' = \frac{s_t}{w_{sat}} - \frac{s_i}{\ln\left(1+\frac{10^6}{s_r}\right) \times (s_i + s_r) \times 1.31^m} \quad (4)$$

$$s_t = \frac{w_i}{\ln\left(\frac{s_p}{s_i}\right)} \quad (5)$$

In above equations, the fitting parameters *a*, *m*, and *n* are determined using a non-linear least squares regression method. In Equation 5, s_p is the intersection of the tangent line to the inflection point with the horizontal axis. The Fredlund and Xing equation requires estimation of four key parameters namely, saturated gravimetric water content (w_{sat}), water content at the inflection point (w_i), suction at the inflection point (s_i), and residual soil suction (s_r) as shown also in Figure 13. The estimated values for these parameters obtained from DT and DTE tests

are given in Table 5. Note that an accurate estimation of the s_r values were not possible due to unavailability of data points for high suctions close to the residual suction, hence this value was assumed as 7 MPa, a value that provides the best curve fitting results to the experimental data in low suction ranges.

It is worth mentioning here that other and more complex sets of curve fitting equations can be found in the literature. For instance, Fredlund and Houston (2013) proposed an equation for curve fitting the experimental SWRC data of soils that undergo significant volume changes with change in suction, by incorporating the shrinkage curve information into the Equation 1. However, as mentioned earlier, to avoid complexity in the proposed method, in this study the simpler version of curve fitting equations was considered. Furthermore, the LC material used in this study was reported in Bagheri and Rezania (2021) to have a slight volume variation with increase in suction to the maximum capacity of the HCTs (i.e. 2.0 MPa), hence justifying the use of the Fredlund and Xing (1994) equation.

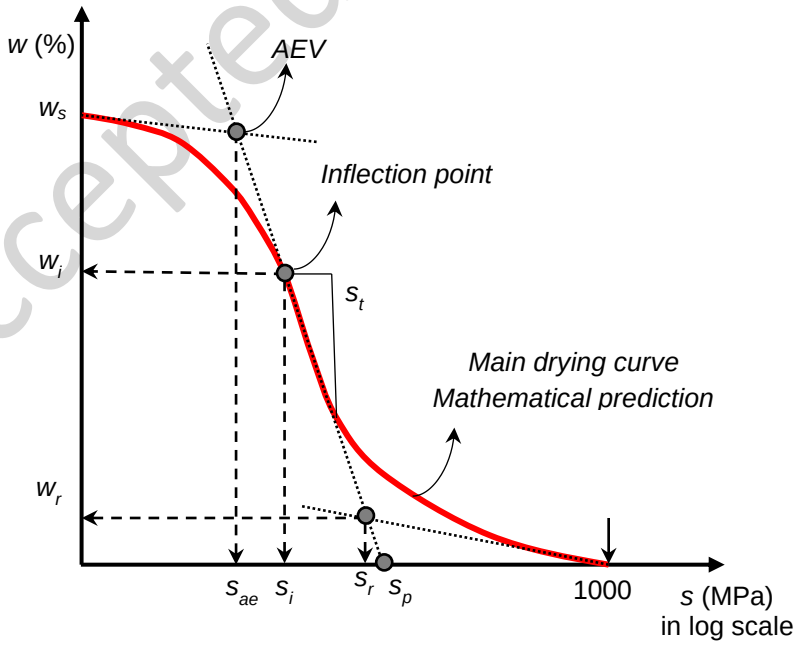

Figure 13. Definitions of the parameters of Fredlund and Xing equation in SWRC-*w* space

Table 5. Input parameters for Fredlund and Xing equation

Test	w_{sat} (%)	w_i (%)	s_i (kPa)
DT1-01-FM	39.72	37.27	258
DT1-04-SP		36.74	316
DT2-05-DP	39.14	36.93	290
DT2-08-AF		36.83	290
DT3-10-TX	39.67	37.13	340
DT3-11-TD		36.72	395
DTE1-01-FM	39.27	36.61	414
DTE1-04-SP		36.64	402
DTE2-05-DP	39.75	36.51	399
DTE2-08-AF		36.13	452
DTE3-10-TX	39.64	36.11	436
DTE3-11-TD		36.08	449

Figure 14 presents the best-fit curves to the experimental data obtained from DT and DTE tests. The best-fit curves are denoted by a 'CF' added to the test codes. Overall, providing the accurate estimation of the input parameters, the Equation 1 was found to be capable of producing best-fit curves that are closely matching the experimental data. The best fit curves to the DT tests somewhat diverge, whereas almost all of the best-fit curves to the DTE test results coincide on the desorption curve at least from the onset of desaturation to the point corresponding approximately to s = 2 MPa. From this point, notable differences in the extrapolated suctions corresponding to given water contents along the main drying paths of the extended SWRCs for DT and DTE tests are observed (Figure 15). For instance, suctions corresponding to w = 22% vary in a range of 3.9 – 4.5 MPa and 4.8 – 5.8 MPa respectively for the best-fit curves to the DTE and DT tests. It should be noted that this method may not be the

most practical approach, and therefore, the use of indirect suction measurement methods, such as filter paper or psychrometer, for measurement of suctions beyond the capacity of the HCTs seems to be inevitable.

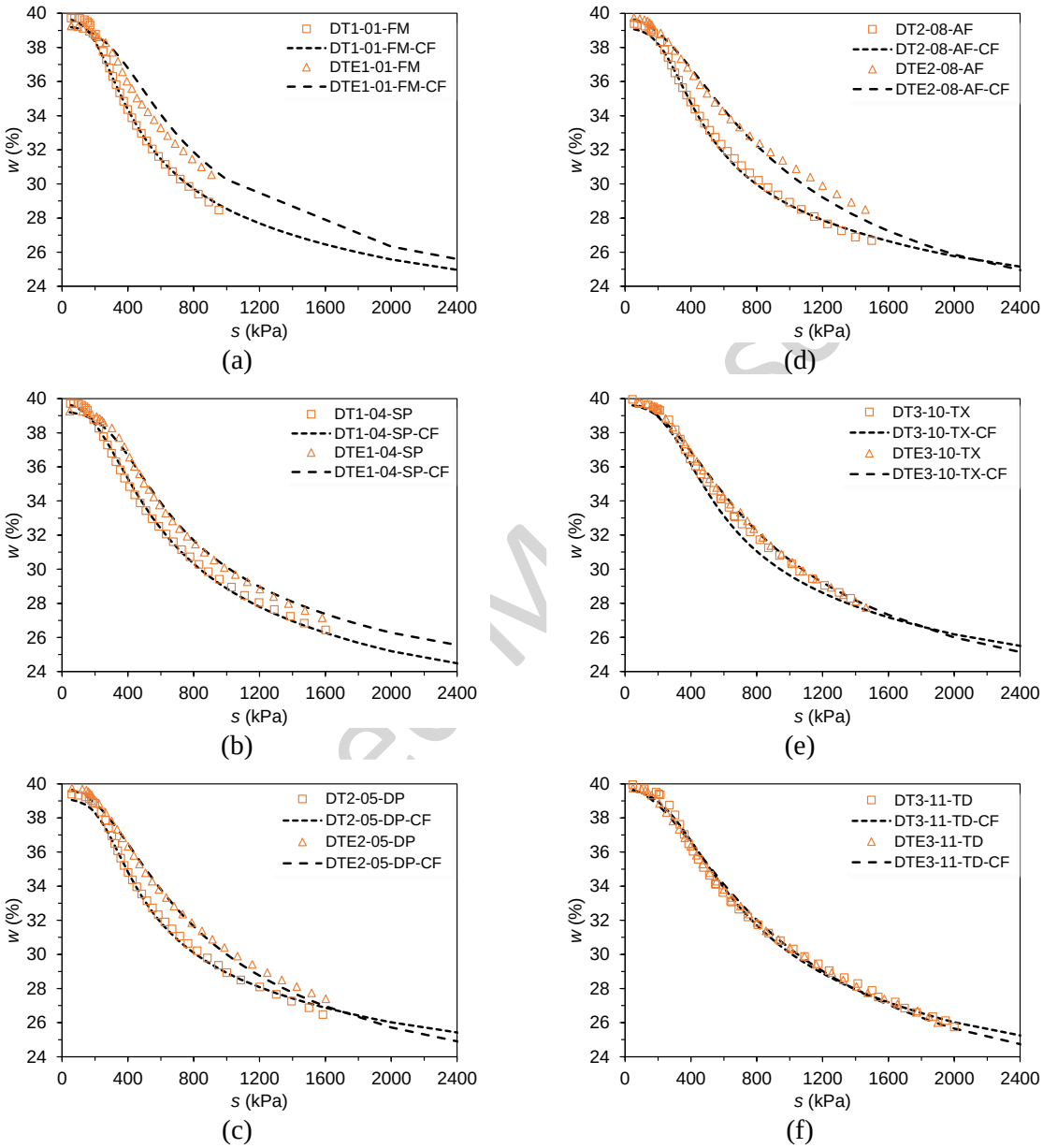

Figure 14. Best-fit curves to the experimental data obtained from DT and DTE tests for different HCT types: (a) FM; (b) SP; (c) DP; (d) AF; (e) TX; and (f) TD

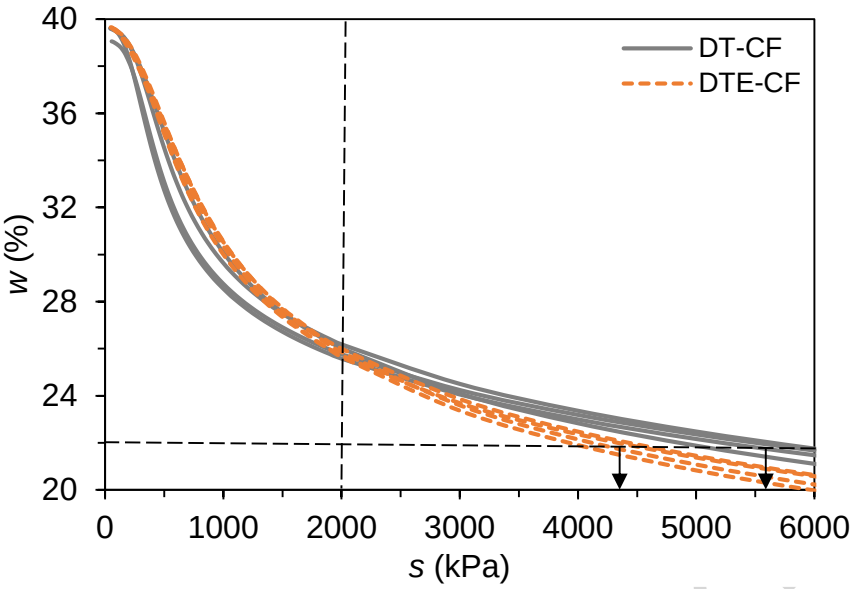

Figure 15. Comparison of best-fit curves to the experimental data obtained from DT and DTE tests

Conclusion

The SWRC of the reconstituted LC specimens over the main drying path were determined using new Warwick HCTs, with enhanced cavitation resistance, following continuous drying procedures with and without soil moisture evaporation rate control. The following conclusions can be drawn;

- In contrast to the works of Cunningham (2000) and Boso et al. (2003) that report the independency of the tensiometric-based SWRCs to the evaporation rate using the dynamic method, it was found that the evaporation rate can influence the measured s_{ae}.
- Generally, the AEVs obtained from DTE tests (with evaporation rate control) were higher than the DT tests (without evaporation rate control) with a mean difference of approximately 39 kPa (or 16% of the mean AEV measured in DT tests), mainly due to the extended pressure equalisation time during suction measurements in DTE tests.
- The SWRCs measured in DTE tests generally exhibit higher suctions than DT tests at a given water content. This observation is more evident for measurements recorded by FM, SP, DP, and AF tensiometers.

- The higher t_{max} values observed during DTE tests can be due to the delayed air diffusion process caused by a reduction in evaporation rate and slowing down the specimen's desaturation and transition from quasi-saturated to partially saturated state.
- The Fredlund and Xing (1994) equation is capable of producing relatively accurate best-fit curves to the experimental data and extrapolation of the water retention behaviour at high suctions given that the input parameters are accurately estimated.
- For suctions beyond 2 MPa, the best-fit curves obtained from DTE tests exhibit significantly lower suctions than DT tests at a given water content. This finding implies that such curve fitting correlations should be used with caution.
- In comparison to the other conventional testing methods, DTE technique can be reliably used for measurement of SWRC and in a significantly shorter period.

Notations

The following symbols are used in this paper:

e_0	initial void ratio
G_s	specific gravity
LL	liquid limit
PI	plasticity index
PL	plastic limit
R_a	surface roughness parameter
s	soil suction
s_{ae}	suction at air-entry
s_i	suction at inflection point
s_{max}	maximum attainable suction
s_r	residual soil suction
S_r	degree of saturation
t_{max}	maximum measurement duration
w	gravimetric water content
w_f	final water content
w_i	water content at inflection point
w_{sat}	gravimetric water content at saturation
Δm_w	evaporated mass of water
Δt	test duration
θ	volumetric water content
AEV	air-entry value
AF	anti-fog agent
DP	diamond paste polishing
DT	dynamic test without evaporation rate control
DTE	dynamic test with evaporation rate control
FE	free evaporation test
FM	face-milling
HCT	high-capacity tensiometer
LC	London clay
SP	silicon carbide abrasive paper
SWRC	soil water retention curve
TD	Titanium Dioxide
TX	Triton X-100
WT	Warwick tensiometer

References

Bagheri M (2018) Experimental investigation of the time- and rate-dependent behaviour of unsaturated clays. Ph.D. thesis, University of Nottingham.

Bagheri M and Rezania M (2021) Geological and geotechnical characteristics of London clay from the Isle of Sheppey. Geotechnical and Geological Engineering, 39: 1701-1713, https://doi.org/10.1007/s10706-020-01572-3

Bagheri M, Mousavi Nezhad M and Rezania M (2020) A CRS oedometer cell for unsaturated and non-isothermal tests. Geotechnical Testing Journal 43(1): 20-37, https://doi.org/10.1520/GTJ20180204

Bagheri M, Rezania M and Mousavi Nezhad M (2018) Cavitation in High-Capacity Tensiometers: Effect of Water Reservoir Surface Roughness. Geotechnical Research 5(2): 81-95, https://doi.org/10.1680/jgere.17.00016.

Bagheri M, Rezania M and Mousavi Nezhad M (2019) Rate dependency and stress relaxation of unsaturated clays. International Journal of Geomechanics 19(12): 04019128, https://doi.org/10.1061/(ASCE)GM.1943-5622.0001507

Boso M, Romero E and Tarantino A (2003) The use of different suction measurement techniques to determine water retention curves. In Proceedings of an International Conference on From Experimental Evidence towards Numerical Modeling of Unsaturated Soils (Schanz T (ed)). Springer, Weimar, Germany, pp. 171-181.

Chen R, Liu J, Li JH and Ng CW (2015) An integrated high-capacity tensiometer for measuring water retention curve continuously. Soil Science Society of America Journal, 79: 943-947, doi:10.2136/sssaj2014.11.0438n

Cunningham MR (2000) The mechanical behaviour of a reconstituted unsaturated soil. Ph.D. Thesis, Imperial College University.

Fredlund DG and Rahardjo H (1993) Soil mechanics for unsaturated soils, John Wiley & Sons, New York.

Fredlund DG and Xing A (1994) Equations for the soil-water characteristic curve. Canadian Geotechnical Journal 31: 521-532.

Fredlund, D. G. & Houston, S. L. (2013). Interpretation of soil-water characteristic curves when volume change occurs as soil suction is changed. In: Advances in Unsaturated Soils: Proceedings of the 1st Pan-American Conference on Unsaturated Soils, PanAmUNSAT 2013, Taylor & Francis Group, London, ISBN: 978-041562095-6, Volume: 1, 15-31.

Lourenço SDN, Gallipoli D, Toll DG et al (2011) A new procedure for the determination of the soil water retention curves by continuous drying using high suction tensiometers. Canadian Geotechnical Journal 48: 327-335.

Marinho FAM and Teixeira PF (2009) The use of high capacity tensiometer for determining the soil water retention curve. Soil and Rocks Journal 32(2): 91-96.

Munoz-Castelblanco JA, Pereira JM, Delage P and Cui YJ (2012) The water retention properties of a natural unsaturated loess from northern France. Geotechnique 62(2): 95-106, http://dx.doi.org/10.1680/geot.9.P.084

Noguchi T, Mendes J and Toll DG (2012) Comparison of soil water retention curve obtained by filter paper, high capacity suction probe and pressure plate. In 5th Asia-Pacific Conference on Unsaturated Soils 2012. Vol. 1. NY Curran Associates, Inc. 2012. p. 368-373.

Pagano A, Tarantino A, Bagheri M et al (2016) An experimental investigation of the independent effect of suction and degree of saturation on very small-strain stiffness of unsaturated sand. E3S Web of Conferences 9: 14015 https://doi.org/10.1051/e3sconf/20160914015

Rezania M, Bagheri M and Mousavi Nezhad M (2020) Creep and consolidation of a stiff clay under saturated and unsaturated conditions. Canadian Geotechnical Journal 57(5): 728-741, https://doi.org/10.1139/cgj-2018-0398

Toll DG, Asquith JD, Fraser A, Hassan AA, Liu G, Lourenço SDN, Mendes J, Noguchi T, Osinski P, Stirling R (2015) Tensiometer techniques for determining soil water retention curves. Asia-Pacific Conference on Unsaturated Soil, Guilin, China, doi: 10.1201/b19248-4